

# Synthesis of $\text{Lu}_{2.94}\text{Ce}_{0.06}\text{MgAl}_3\text{SiO}_{12}$ phosphor and its photoluminescent properties

Jung-Il Lee, Tae Wan Kim, Ji Young Shin and Jeong Ho Ryu<sup>†</sup>

*Department of Materials Science and Engineering, Korea National University of Transportation, Chungju 380-702, Korea*

(Received June 5, 2015)

(Revised June 11, 2015)

(Accepted June 15, 2015)

**Abstract** A novel  $\text{Ce}^{3+}$  doped  $\text{Lu}_3\text{MgAl}_3\text{SiO}_{12}$  phosphor ( $\text{Lu}_{2.94}\text{Ce}_{0.06}\text{MgAl}_3\text{SiO}_{12}$ ) was successfully synthesized by a conventional solid-state reaction at 1450°C for 5 h. The crystal structure of the synthesized phosphor powder was characterized by X-ray diffraction and Rietveld refinement. The prepared phosphor powder showed a broad peak at 550 nm, and the temperature dependence on photoluminescence properties of the prepared  $\text{Lu}_{2.94}\text{Ce}_{0.06}\text{MgAl}_3\text{SiO}_{12}$  phosphor was investigated from 300 to 525 K. The activation energy for thermal quenching was determined by Arrhenius fitting. The experimental results clearly indicate that prepared  $\text{Lu}_{2.94}\text{Ce}_{0.06}\text{MgAl}_3\text{SiO}_{12}$  phosphor has great potential for a down-conversion yellow phosphor in white light-emitting diodes.

**Key words**  $\text{Lu}_{2.94}\text{Ce}_{0.06}\text{MgAl}_3\text{SiO}_{12}$ , Phosphor, Photoluminescence, Thermal quenching

## 1. Introduction

The first commercially available white LED (light emitting diodes) based on phosphors was produced by Nichia Co., which was also first to manage to make the blue LED. Nichia used a blue light emitting gallium indium nitride (GaInN) chip coated with yellow phosphor  $\text{Y}_3\text{Al}_5\text{O}_{12}:\text{Ce}^{3+}$ , well known as YAG :  $\text{Ce}^{3+}$  [1]. With the perspective of a highly efficient light source, the LED market will have an enormous growth and the white LED will be a likely candidate for the replacement of the light bulb. However, the color temperature of YAG :  $\text{Ce}^{3+}$  phosphor used for luminescence converting LED is too high to use in warm white LED application because of lacking red component [2]. The color temperature of warm white, cool white and daylight white area round 3300 K, 4200 K and 6400 K, respectively. For general indoor lighting application, “warmer” white light is recommended [3].

To meet the requirements for general illumination lighting, two major modifications have been developed. One is the modification of the YAG : Ce system, including co-doping rare earths or transition metal ions, which can increase red component [4]. The problem is the enhancement of the red component efficiency is not obvious, and almost all bright and thermal stability of

modification YAG : Ce are obviously declined. The other is exploring novel red phosphors which are usually based on  $\text{Eu}^{2+}$  doped nitrides phosphors [5]. However, these phosphors require critical preparation conditions like high temperature, high pressure and expensive raw materials. Besides, they have to be blended with YAG : Ce phosphor to make white lamps, possibly leading to variations during lamp manufacturing.

It is possible and valid to modify the typical garnet composition to obtain a significant red-shift emission spectrum, because the energy position of the lowest  $\text{Ce}^{3+}$  5d level could be justified by changing the crystal field splitting and the covalency of  $\text{Ce}^{3+}-\text{O}^{2-}$ . In addition, the  $\text{Ce}^{3+}$  doped garnet host lattices are the only oxide phosphors that could absorb blue light and emit from yellow to orange-red light [6]. In a practical sense, phosphors should not only have redder spectra for lower correlated color temperature (CCT) and high color rendering index (CRI) but also high quantum efficiency (QE) and high thermal stability for warm white LED phosphors. In this study, we present a solid-state synthesis inducing  $\text{Mg}^{2+}-\text{Si}^{4+}$  pairs into  $\text{Lu}^{3+}$  based garnet, and discuss its crystal structure. Photoluminescence at room temperature and thermal quenching at high temperatures are investigated.

## 2. Experimental

The  $\text{Ce}^{3+}$  doped  $\text{Lu}_3\text{MgAl}_3\text{SiO}_{12}$  ( $\text{Lu}_{2.94}\text{Ce}_{0.06}\text{MgAl}_3\text{SiO}_{12}$ )

<sup>†</sup>Corresponding author  
Tel: +82-43-841-5384  
Fax: +82-43-841-5380  
E-mail: jhryu@ut.ac.kr

was synthesized by the conventional solid-state reaction method.  $\text{Lu}_2\text{O}_3$  (Kanto Chemical, 99.99 %),  $\text{CeO}_2$  (Kanto Chemical, 99.99 %),  $\text{MgO}$  (Kanto Chemical, 99.99 %), and  $\text{SiO}_2$  (Kanto Chemical, 99.9 %) were used as starting materials. Cerium concentration was fixed at 6.0 mol%. All starting materials were weighted out as the desired stoichiometry and thoroughly mixed using an agate mortar with small amount of ethanol. The mixture was first calcined at  $800^\circ\text{C}$  for 2 h using alumina crucible in air then fired at  $1450^\circ\text{C}$  for 5 h in  $\text{N}_2$  atmosphere. Finally, the phosphor sample was cooled to room temperature in the furnace and ground with an agate mortar. The fired phosphor sample ( $\text{Lu}_{2.94}\text{Ce}_{0.06}\text{MgAl}_3\text{SiO}_{12}$ ) showed yellow body color.

Powder X-ray diffraction (XRD) data were collected on a Bruker D8 powder X-ray diffractometer with  $\text{Cu K}\alpha$  radiation ( $\lambda = 1.54178 \text{ \AA}$ ) operating 40 kV and 30 mA. Step scans were performed from  $60^\circ$  to  $110^\circ$  ( $2\theta$ ) with as step size of  $0.01^\circ$ . Refined lattice parameters of XRD patterns were fit by Rietveld refinements using FULLPROF program [7]. Microstructure and surface morphology of the  $\text{Lu}_{2.94}\text{Ce}_{0.06}\text{MgAl}_3\text{SiO}_{12}$  powder were observed by scanning electron microscope (Hitachi S-4800, Japan). Photoluminescence excitation (PLE) and emission (PL) spectra were measured by fluorescence spectrometer (Scinco FS-2) system in a temperature range of 25 and  $275^\circ\text{C}$  using a 450 W xenon lamp as an excitation source.

### 3. Results and Discussion

Crystallographic information of the  $\text{Lu}_{2.94}\text{Ce}_{0.06}\text{MgAl}_3\text{SiO}_{12}$  phosphor is one of the important factors affecting the photoluminescence properties, which closely relates with the crystal field strength surrounding the ions in each crystallographic sites. Crystallographic data of the  $\text{Lu}_{2.94}\text{Ce}_{0.06}\text{MgAl}_3\text{SiO}_{12}$  was extracted by the Rietveld refinements of the XRD profile of the  $\text{Lu}_{2.94}\text{Ce}_{0.06}\text{MgAl}_3\text{SiO}_{12}$ , as shown in Fig. 1. Approximate structural parameters for  $\text{Lu}_{2.94}\text{Ce}_{0.06}\text{MgAl}_3\text{SiO}_{12}$  calculation was obtained from the data, previously reported for  $\text{Lu}_3\text{Al}_5\text{O}_{12}$  (LuAG; JCPDS 73-1368) [8]. The LuAG was decided as the initial structure model for  $\text{Lu}_{2.94}\text{Ce}_{0.06}\text{MgAl}_3\text{SiO}_{12}$  calculation due to the similarity of the crystal structure; both of them belong to the garnet structure family (cubic, space group #230), with the general formula  $(\text{A}_3)[\text{B}_2]\langle\text{C}_3\rangle\text{O}_{12}$ , where ( ), [ ] and  $\langle \rangle$  denote dodecahedral, octahedral and tetrahedral coordination, respectively [9]. In the crystal structure of LuAG,  $\text{Lu}^{3+}$  ions and  $\text{Al}^{3+}$  occupy the dodecahedral and octahedral/tetra-

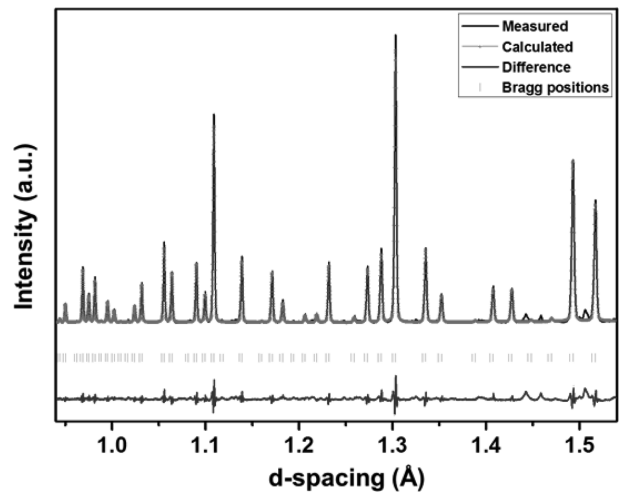


Fig. 1. Rietveld refinements of XRD patterns of  $\text{Lu}_{2.94}\text{Ce}_{0.06}\text{MgAl}_3\text{SiO}_{12}$  phosphor with positions of all the reflection (orange) and a difference profile (blue); Measured (black) and calculated (red).

Table 1  
Refined structural parameters for  $\text{Lu}_{2.94}\text{Ce}_{0.06}\text{MgAl}_3\text{SiO}_{12}$  phosphor

Atom	Wyckoff	x	y	z	Occupancy
Lu	24c	0.125	0	0.25	2.77
Ce	24c	0.125	0	0.25	0.22
Al1	16a	0	0	0	1.01
Mg	16a	0	0	0	1.01
Al2	24d	0.375	0.25	0	1.98
Si	24d	0.375	0.25	0	0.98
O	96h	-0.033	0.053	0.153	12.00

hedral sites, respectively. On the other hand, in the crystal structure of LCMAS, dodecahedral sites are occupied by  $\text{Lu}^{3+}$  and  $\text{Ce}^{3+}$ . Also,  $\text{Mg}^{2+}/\text{Al}^{3+}$  and  $\text{Al}^{3+}/\text{Si}^{4+}$  occupy octahedral and tetragonal sites, respectively.

Refined structure parameters of  $\text{Lu}_{2.94}\text{Ce}_{0.06}\text{MgAl}_3\text{SiO}_{12}$  are listed in Table 1. The refinement confirmed that  $\text{Lu}_{2.94}\text{Ce}_{0.06}\text{MgAl}_3\text{SiO}_{12}$  is cubic with space group  $Iad$ , and lattice parameter is refined as  $11.942 \text{ \AA}$ . Wyckoff sites of 24c, 16a, 24d and 96h are occupied by Lu/Ce, Mg/Al1, Si/Al2 and O, respectively. As shown in Table 1, the calculated occupancies of ions from XRD pattern are quite well matched with experimental. The comparison of lattice parameters and cell volume between LuAG and  $\text{Lu}_{2.94}\text{Ce}_{0.06}\text{MgAl}_3\text{SiO}_{12}$  is shown in the Table 2. The deviation of lattice parameter is  $0.0359 \text{ \AA}$  and the deviation of oxygen atomic coordinates (x, y, z) is  $-0.0033$ ,  $-0.0006$  and  $0.0023$ , respectively.

Cell volume and lattice parameters of  $\text{Lu}_{2.94}\text{Ce}_{0.06}\text{MgAl}_3\text{SiO}_{12}$  are larger than that of LuAG ( $11.9064 \text{ \AA}$ ) because the smaller  $\text{Al}^{3+}$  is partly substituted by larger  $\text{Mg}^{2+}$  in the octahedral sites. Also, smaller  $\text{Lu}^{3+}$  is partly

Table 2  
The lattice parameters and the oxygen atomic coordinates obtained by Rietveld refinement

Sample	Lattice	Volume ( $\text{\AA}^3$ )	Oxygen atomic coordinates			$R_p$	$R_{wp}$
			x	y	z		
LuAG	11.906	1687.5	-0.0294	0.0538	0.1510	0.046	-
$\text{Lu}_{2.94}\text{Ce}_{0.06}\text{MgAl}_3\text{SiO}_{12}$	11.942	1703.2	-0.0327	0.0532	0.1533	0.104	0.131

replaced by larger  $\text{Ce}^{3+}$  which results in the increase of the cell parameters and volume of  $\text{Lu}_{2.94}\text{Ce}_{0.06}\text{MgAl}_3\text{SiO}_{12}$ . In the same manner, smaller lattice constant of the  $\text{Lu}_{2.94}\text{Ce}_{0.06}\text{MgAl}_3\text{SiO}_{12}$  than  $\text{Y}_3\text{Al}_5\text{O}_{12}$  (YAG; 12.066  $\text{\AA}$ ) is likely due to the smaller ionic size of  $\text{Lu}^{3+}$  than  $\text{Y}^{3+}$  in the dodecahedral sites [10]. The lattice parameters of  $\text{Lu}_{2.94}\text{Ce}_{0.06}\text{MgAl}_3\text{SiO}_{12}$  between those of LuAG and YAG imply that a solid solution of  $\text{Lu}_{2.94}\text{Ce}_{0.06}\text{MgAl}_3\text{SiO}_{12}$  successfully formed. However, small amount of secondary phases was observed as shown in Fig. 1. The formation of the secondary phases might be possibly due to the reducing conditions during heating process, which leads to the local oxygen deficiency for the formation of the secondary phases.

Fig. 2 displays the crystal structure of  $\text{Lu}_{2.94}\text{Ce}_{0.06}\text{MgAl}_3\text{SiO}_{12}$  phosphor based on the results of refinements. As explained above, Lu/Ce, Mg/Al1, Si/Al2, and O are randomly distributed on the dodecahedral, octahedral, and tetrahedral sites, respectively. Every  $(\text{Ce/Lu})\text{O}_8$  dodecahedron is surrounded by four  $(\text{Ce/Lu})\text{O}_8$  dodecahedra, four  $(\text{Mg/Al1})\text{O}_6$  octahedra and six  $(\text{Si/Al2})\text{O}_4$  tetrahedra. The result implies that every coordination  $\text{O}^{2-}$  of  $\text{Ce}^{3+}$  is shared by four cations (two  $\text{Lu}^{3+}$ , one Mg/Al1 and one Si/Al2), which shows that the photoluminescence properties of  $\text{Lu}_{2.94}\text{Ce}_{0.06}\text{MgAl}_3\text{SiO}_{12}$  phosphor is affected by  $(\text{Ce/Lu})\text{O}_8$  as well as  $(\text{Mg/Al1})\text{O}_6$  and  $(\text{Si/Al2})\text{O}_4$  [11].

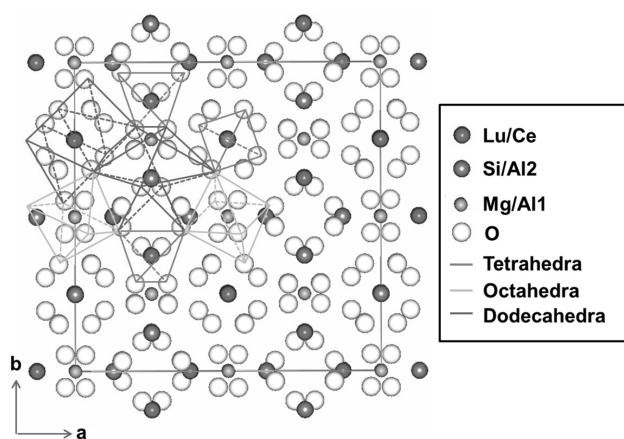


Fig. 2. Simulated crystal structure of  $\text{Lu}_{2.94}\text{Ce}_{0.06}\text{MgAl}_3\text{SiO}_{12}$  phosphor.

For investigation of particle size and morphology, SEM images of the  $\text{Lu}_{2.94}\text{Ce}_{0.06}\text{MgAl}_3\text{SiO}_{12}$  phosphor is shown in Fig. 3(a). Fig. 3(a) shows homogeneous and irregular particle shape with diameter of 1~5  $\mu\text{m}$ . The EDX spectra in Fig. 3(b) obtained from  $\text{Lu}_{2.94}\text{Ce}_{0.06}\text{MgAl}_3\text{SiO}_{12}$  particles show the presence of Lu, Ce, Mg, Al, Si and O with an approximately correct stoichiometry and the absence of any impurity. It can be seen the particle surface is not smooth and some pits exist, this is owing to the agglomerate by lots of small particles to form a big particle in the calcination process. In addition, the average particle size is found to be less than 10  $\mu\text{m}$ , which is suitable for the practical application.

The room temperature Photoluminescence excitation (PLE) and emission (PL) spectra of the  $\text{Lu}_{2.94}\text{Ce}_{0.06}\text{MgAl}_3\text{SiO}_{12}$  phosphor powder heat-treated at 1450 $^\circ\text{C}$  are shown in Fig. 4(a). As expected for a garnet host, the

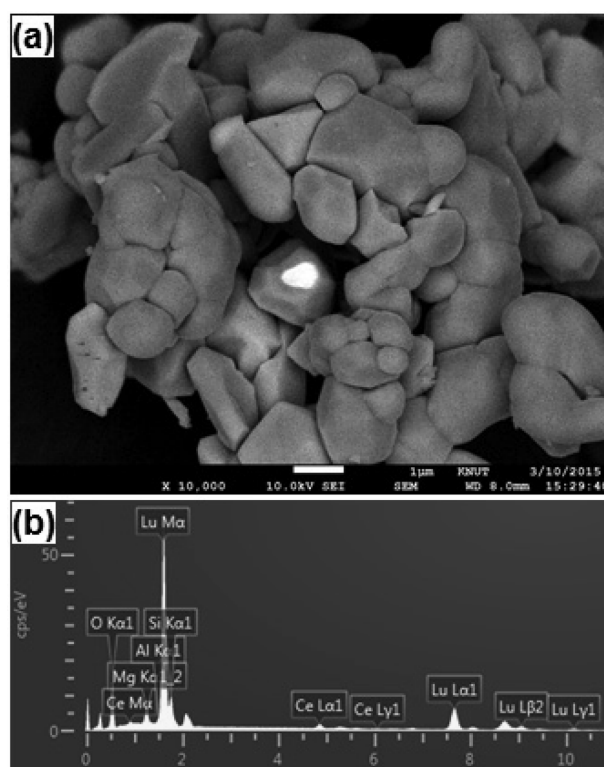


Fig. 3. (a) SEM photograph and (b) EDX profile for the  $\text{Lu}_{2.94}\text{Ce}_{0.06}\text{MgAl}_3\text{SiO}_{12}$  phosphor powder.

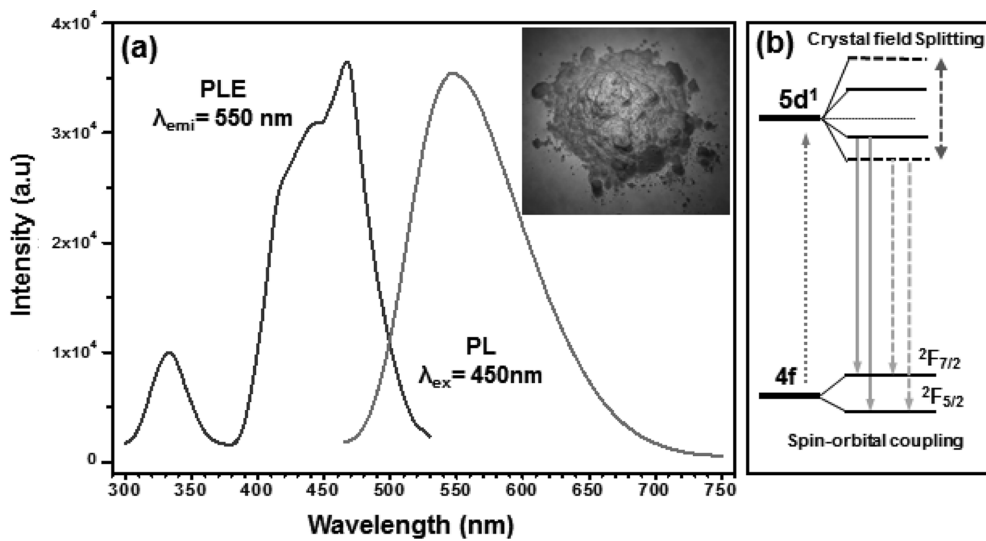


Fig. 4. (a) The room temperature photoluminescence excitation (PLE) and emission (PL) spectra of the  $\text{Lu}_{2.94}\text{Ce}_{0.06}\text{MgAl}_3\text{SiO}_{12}$  phosphor. The inset figure shows the digital photograph for the  $\text{Lu}_{2.94}\text{Ce}_{0.06}\text{MgAl}_3\text{SiO}_{12}$  phosphor. (b) Schematic diagram for electronic energy configuration of  $\text{Ce}^{3+}$  in the  $\text{Lu}_{2.94}\text{Ce}_{0.06}\text{MgAl}_3\text{SiO}_{12}$  phosphor.

lowest  $\text{Ce}^{3+} 4f \leftrightarrow 5d^1$  absorption transition is in the blue spectral region, leading to greenish yellow to orange color. The excitation spectrum of the  $\text{Lu}_{2.94}\text{Ce}_{0.06}\text{MgAl}_3\text{SiO}_{12}$  phosphor powder is shown in the left of Fig. 4. The excitation spectrum exhibit two excitation bands of  $\text{Ce}^{3+}$ , one  $5d$  band near at 450 nm, and the other  $5d$  band level near at 330 nm, which correspond to the two lowest  $5d$  levels of  $\text{Ce}^{3+}$  [12].

The electronic configuration of rare-earth element  $\text{Ce}^{3+}$  is  $[\text{Xe}]4f^15d^0$ . The wide absorption band and the emission peaks of  $\text{Ce}^{3+}$  originate from the  $4f \leftrightarrow 5d$  transition. The splitting of the  $\text{Ce}^{3+}$  energy level is induced by the covalency effect (nephelauxetic effect) and the crystal field effect, allowing the PL performance of  $\text{Ce}^{3+}$  to be tuned. The energy configuration of  $\text{Ce}^{3+}$  is shown in Fig. 4(b). The PLE spectra show a broad excitation peak at 450 nm, which is attributed to the absorption of the allowed transition from  $4f^1$  to  $5d^1$  of  $\text{Ce}^{3+}$ . This makes  $\text{Lu}_{2.94}\text{Ce}_{0.06}\text{MgAl}_3\text{SiO}_{12}$  phosphor suitable for fabrication with commercial blue LED chips. The PL spectra show an asymmetric emission peak at around 550 nm under excitation at 450 nm. The broad peak is a combination of two peaks, which derive from the energy transfer of  $5d^1 \rightarrow {}^2F_{5/2}$  and  ${}^2F_{7/2}$  of  $\text{Ce}^{3+}$ , respectively. The splitting of the  $f_1$  ground state of  $\text{Ce}^{3+}$  into  ${}^2F_{5/2}$  and  ${}^2F_{7/2}$  is due to the spin-orbit coupling effect [13].

Thermal quenching property is one of the most important technological parameters for phosphors applied to white-LEDs. The temperature dependent PL properties of the prepared  $\text{Lu}_{2.94}\text{Ce}_{0.06}\text{MgAl}_3\text{SiO}_{12}$  phosphor powder was investigated in a temperature range from 300 to

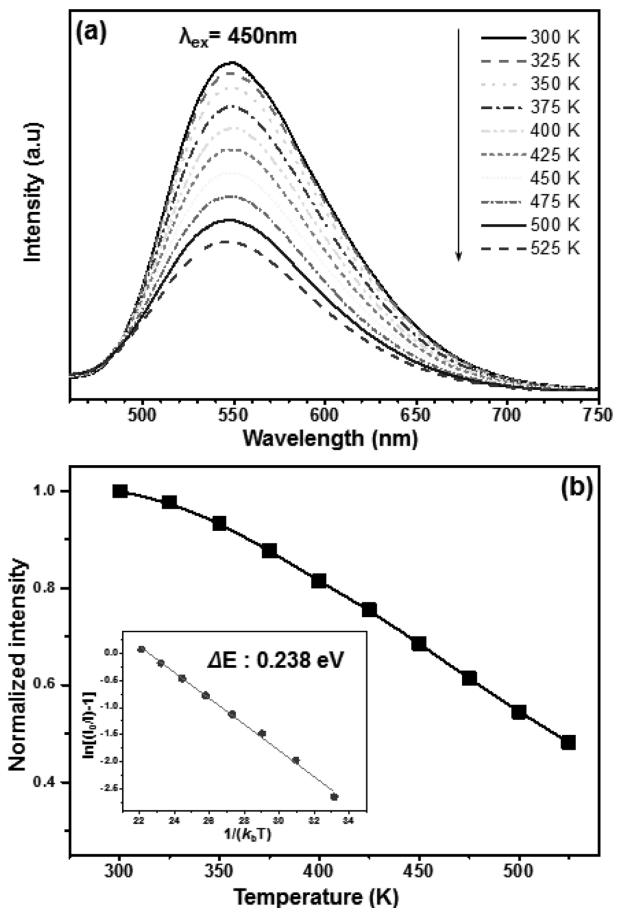


Fig. 5. (a) The emission spectra measured with increasing temperature from 300 to 525 K for the  $\text{Lu}_{2.94}\text{Ce}_{0.06}\text{MgAl}_3\text{SiO}_{12}$  phosphor powder. (b) Temperature dependence of emission intensity in the temperature range. The graph in the inset depicts an Arrhenius fitting of the emission intensity in the measuring temperature range with calculated activation energy for thermal quenching ( $\Delta E$ ).

525 K and shown in Fig. 5(a). At 425 K, the emission intensity was 76 % of those measured at room temperature which was 10 % higher than that of the commercial Y<sub>3</sub>Al<sub>5</sub>O<sub>12</sub> : Ce<sup>3+</sup> (YAG : Ce, P46-y3) phosphor. Upon heating the Lu<sub>2.94</sub>Ce<sub>0.06</sub>MgAl<sub>3</sub>SiO<sub>12</sub> phosphor powder, the dwindling of emission intensity and broadening of bandwidths (FWHM) are shown clear, which can be explained by the thermal quenching in the configurational coordinate model [14]. The low potential curve and the high one represent the total energy of the ground state of 4*f* and the excited state of 5*d*<sup>1</sup>, respectively. The equilibrium positions of the two states are different from each other because of the different spatial distribution of the electron orbitals. The excited luminescent center is thermally activated through phonon interaction, and then thermally released through the crossing point between the excited state and the ground state in the configurational coordinate diagram. This non-radiative transition induced by thermal activation is strongly dependent on temperature, which results in the thermal quenching of the emission intensity. In addition, the electron-phonon interaction resulted from increased population density of phonon broadens FWHM of emission spectra at high temperature [15].

Fig. 5(b) displays decrease of normalized emission intensity for prepared Lu<sub>2.94</sub>Ce<sub>0.06</sub>MgAl<sub>3</sub>SiO<sub>12</sub> phosphor as a function of measuring temperature. In order to further understand the temperature dependence of PL intensity and to determine the activation energy for thermal quenching, the Arrhenius equation was fitted to the thermal quenching data as shown in the inset of Fig. 5(b). According to the classical theory of thermal quenching, the temperature-dependent emission peak intensity can be described by the expression [16],

$$I(T) = \frac{I_0}{1 + A \exp\left(\frac{-\Delta E}{k_B T}\right)} \quad (1)$$

where  $I_0$  is the initial intensity,  $I(T)$  is the intensity at a given temperature  $T$ ,  $A$  is a constant,  $\Delta E$  is the activation energy for thermal quenching, and  $k_B$  is Boltzmann's constant. The graph in the inset of Fig. 6(b) plots  $\ln[(I_0/I) - 1]$  versus  $1/(k_B T)$  and gives a straight line up to  $T = 525$  K. The best fit following Eq. (1) gives activation energy ( $\Delta E$ ) of 0.238 eV.

#### 4. Summary

In this work, Ce<sup>3+</sup> doped Lu<sub>3</sub>MgAl<sub>3</sub>SiO<sub>12</sub> (Lu<sub>2.94</sub>Ce<sub>0.06</sub>

MgAl<sub>3</sub>SiO<sub>12</sub>) was successfully synthesized by a conventional solid-state reaction at 1450°C for 5 h. XRD Rietveld refinement results show that the Lu<sub>2.94</sub>Ce<sub>0.06</sub>MgAl<sub>3</sub>SiO<sub>12</sub> phosphor has a garnet structure, and Ce<sup>3+</sup> ions occupy Lu<sup>3+</sup> sites on the dodecahedral sites, and Si and Al<sub>2</sub> are randomly distributed on the octahedral sites, Mg and Al<sub>1</sub> are randomly distributed on the tetrahedral sites. The photoluminescence excitation (PLE) and emission (PL) spectra showed that this novel garnet phosphor can be excited efficiently at 450 nm and it can emit yellow color with high luminescence intensity. Temperature dependence on PL property of the prepared Lu<sub>2.94</sub>Ce<sub>0.06</sub>MgAl<sub>3</sub>SiO<sub>12</sub> phosphor powder was investigated from 300 to 525 K and showed better thermal stability than the commercial YAG : Ce phosphor powder. By fitting the temperature dependent PL data based on the classical thermal quenching theory, the activation energy ( $\Delta E$ ) for thermal quenching were determined to be 0.238 eV.

#### Acknowledgement

This research was supported by a grant from the School of Convergence Program of Ministry of Education.

#### References

- [1] S.M. Hwang, J.B. Lee, S.H. Kim and J.H. Ryu, "A review on inorganic phosphor materials for white LEDs", *J. Kor. Cryst. Growth and Technol.* 22 (2012) 233.
- [2] C.C. Lin, Y.S. Zheng, H.Y. Chen, C.H. Ruan, G.W. Xiao and R.S. Liu, "Improving optical properties of white LED fabricated by a blue LED chip with yellow/red phosphors", *J. Electrochem. Soc.* 157 (2010) H900.
- [3] A.A. Setlur, W.J. Heward, Y. Gao, A.M. Srivastava, R.G. Chandran and M.V. Shankar, "Crystal chemistry and luminescence of Ce<sup>3+</sup>-doped Lu<sub>2</sub>CaMg<sub>2</sub>(Si,Ge)<sub>3</sub>O<sub>12</sub> and its use in LED based lighting", *Mater. Chem.* 18 (2006) 3314.
- [4] J. Zhou, Y. Teng, X. Liu, S. Ye, Z. Ma and J. Qiu, "Broadband spectral modification from visible light to near-infrared radiation using Ce<sup>3+</sup>-Er<sup>3+</sup> codoped yttrium aluminium garnet", *Phys. Chem. Chem. Phys.* 12 (2010) 13759.
- [5] B. Lee, S. Lee, H.G. Jeong and K.-S. Sohn, "Solid-state combinatorial screening of (Sr,Ca,Ba,Mg)<sub>2</sub>Si<sub>5</sub>N<sub>8</sub> : Eu<sup>2+</sup> phosphors", *ACS Comb. Sci.* 13 (2011) 154.
- [6] W. Zhou, X. Ma, M. Zhang, Y. Luo and Z. Xia, "Synthesis and photoluminescence properties of green-emitting Lu<sub>3</sub>(Al,Sc)<sub>5</sub>O<sub>12</sub> : Ce<sup>3+</sup> phosphor", *Ceram. Int.* 41 (2015) 7140.
- [7] M.T. Caldes, P. Deniard, X.D. Zou, R. Marchand, N. Diot and R. Brec, "Solving modulated structures by X-

- ray and electron crystallography”, *Micron* 32 (2001) 497.
- [ 8 ] F. Euler and J.A. Bruce, “Oxygen coordinates of compounds with garnet structure”, *Acta Cryst.* 19 (1965) 971.
- [ 9 ] M. Shang, J. Fan, H. Lian, Y. Zhang, D. Geng and J. Lin, “A double substitution of  $Mg^{2+}$ - $Si^{4+}/Ge^{4+}$  for  $Al_{(1)}^{3+}$ - $Al_{(2)}^{3+}$  in  $Ce^{3+}$ -doped garnet phosphor for white LEDs”, *Inorg. Chem.* 53 (2014) 7748.
- [10] Y. Shi, G. Zhu, M. Mikami, Y. Shimomura and Y. Wang, “A novel  $Ce^{3+}$  activated  $Lu_3MgAl_3SiO_{12}$  garnet phosphor for blue chip light-emitting diodes with excellent performance”, *Dalton Trans.* 44 (2015) 1775.
- [11] A. Katelnikovas, H. Bettentrup, D. Uhlich, S. Sakirzhanovas, T. Jüstel and A. Kareiva, “Synthesis and optical properties of  $Ce^{3+}$ -doped  $Y_3Mg_2AlSi_2O_{12}$  phosphors”, *J. Lumin.* 129 (2009) 1356.
- [12] C.C. Lin and R-S. Liu, “Advances in phosphors for light-emitting diodes”, *J. Phys. Chem. Lett.* 2 (2011) 1268.
- [13] J.L. Wu, G. Gundiah and A.K. Cheetham, “Structure-property correlations in Ce-doped garnet phosphors for use in solid state lighting”, *Chem. Phys. Lett.* 441 (2007) 250.
- [14] J.H. Ryu, Y.-G. Park, H.S. Won, S.H. Kim, H. Suzuki, J.M. Lee, C. Yoon, M. Nazarov, D.Y. Noh and B. Tsukerblat, “Luminescent properties of Ca- $\alpha$ -SiAlON :  $Eu^{2+}$  phosphors synthesized by gas-pressured sintering”, *J. Electrochem. Soc.* 155 (2008) J99.
- [15] Y.-F. Wu, Y.-H. Chan, Y.-T. Nien and I.-G. Chen, “Crystal structure and optical performance of  $Al^{3+}$  and  $Ce^{3+}$  codoped  $Ca_3Sc_2Si_3O_{12}$  green phosphors for white LEDs”, *J. Am. Ceram. Soc.* 96 (2013) 234.
- [16] V. Bachmann, C. Ronda and A. Meijerink, “Temperature quenching of yellow  $Ce^{3+}$  luminescence in YAG : Ce”, *Chem. Mater.* 21 (2009) 2077.